IEEE Access
Multidisciplinary | Rapid Review | Open Access Journal

Received February 24, 2020, accepted March 15, 2020, date of publication March 24, 2020, date of current version April 8, 2020.

Digital Object Identifier 10.1109/ACCESS.2020.2982928

An Affine Arithmetic-Based Model of Interval Power Flow With the Correlated Uncertainties in Distribution System

SHIPENG LENG, KAIPEI LIU, XIAOHONG RAN, (Member, IEEE), SHUYAO CHEN, AND XUNYUE ZHANG

School of Electrical Engineering and Automation, Wuhan University, Wuhan 430072, China
Nanchang Power Supply Company, Jiangxi Electric Power Corporation, Nanchang 330077, China

Corresponding author: Xiaohong Ran (xhran@ehu.edu.cn)

This work was supported in part by the National Natural Science Foundation of China under Grant 51607125, in part by the Hubei Natural Science Foundation under Grant 2017CFB521, and in part by the China Postdoctoral Science Foundation under Grant 2016M602351.

ABSTRACT An interval power flow (IPF) method that considers the interval correlations of input random variables is proposed to improve the calculation accuracy of IPF, i.e., as correlated distributed generations (DGs) and some correlated DGs-loads are integrated into distribution system. The interval correlation for input variables is described by parallelogram model (PM), whose shape and size are determined by the interval correlated level. Based on affine arithmetic (AA) method, the IPF is solved through nonlinear optimization instead of traditional interval iterative computations. The optimization model of IPF is established, and the interval correlations of input variables (DGs-DGs and DGs-loads) are added into the IPF optimization problem in the form of additional constraint, to make the power flow solutions, i.e., bus voltage magnitude, voltage angle, active and reactive power of branches, more accurate. Finally, several cases, i.e., numerical case, IEEE33-bus, PG&E69-bus and IEEE118-bus distribution system, not only demonstrate the effectiveness of the proposed method, but also indicate that the IPF results are affected by uncertainty level, and the widths of IPF increase with the increasing of uncertainty level.

INDEX TERMS Affine arithmetic, interval correlation, interval power flow, nonlinear optimization, parallelogram model.

NOMENCLATURE

x_i^c	Midpoint of interval variable x_i
x_i^w	Radius of interval variable x_i
$\rho_{x_i x_j}$	Correlation coefficient between variables x_i and x_j
ε_i	Noise symbol of interval variable x_i
n	System total bus number
PQ	List of PQ-bus
PV	List of PV-bus
G_{ij}	Real part of the bus admittance matrix Y_{ij}
B_{ij}	Imaginary part of the bus admittance matrix Y_{ij}
e_i	Real part of voltage magnitude for ith bus V_i
f_i	Imaginary part of voltage magnitude for ith bus V_i
θ_i	Angle of V_i
ε_i^P	Injected active power noises at the ith bus
ε_i^Q	Injected reactive power noises at the ith bus
nP	List of PQ-bus and PV-bus
$e_{i,0}$	Central value of e_i
$f_{i,0}$	Central value of f_i
e_{ij}^P	Partial deviation of e_i at the jth bus for active power
f_{ij}^P	Partial deviation of f_i at the jth bus for active power
e_{ij}^Q	Partial deviation of e_i at the jth bus for reactive power
f_{ij}^Q	Partial deviation of f_i at the jth bus for reactive power
$P_{i,0}$	Central value of interval active power
$Q_{i,0}$	Central value of interval reactive power
P_{ij}	Active power of the ijth branch
Q_{ij}	Reactive power of the ijth branch

ABBREVIATIONS

PF	Power Flow
IPF	Interval Power Flow
DGs	Distributed Generations
PM	Parallelogram Model
IA	Interval Arithmetic
AA	Affine Arithmetic

The associate editor coordinating the review of this manuscript and approving it for publication was Huaqing Li.

This work is licensed under a Creative Commons Attribution 4.0 License. For more information, see https://creativecommons.org/licenses/by/4.0/

MP Multi-dimensional Parallelepiped
MC Monte Carlo

I. INTRODUCTION

Power Flow (PF) study is one of the most basic tools in power system analysis and is widely used in state estimation, voltage control and security analysis, etc. [1]. With more and more renewable resources, like wind and photovoltaic, and random loads, i.e., electric vehicles, being integrated into distribution system, traditional deterministic PF cannot meet schedule requirements due to uncertainty of input variables, which leads to uncertainty PF. The PF analysis is actually a problem consisting of nonlinear equations. Once the input parameters of PF equations are uncertain, PF solutions can not be represented by only single values but by intervals [2], [3]. The method based on Interval Arithmetic (IA) to analyze PF is called interval power flow (IPF) algorithm, which has been studied for many years but still remains immature because of the nonlinear characteristics of PF.

In the early development of IPF analysis, the main method is to apply the IA of nonlinear equations into PF analysis [4]. In terms of interval iterative method, the Newton iteration [5] is not suitable for the PF calculation, because the interval Jacobi matrix cannot be inverted, which means that iterations cannot be performed. Soon after, Krawczyk-Moore interval iterative method provides an effective algorithm to solve the problem that interval matrix cannot be inverted [6], which often appears in some IPF researches [7], [8]. Krawczyk-Moore method is useful to solve uncertain nonlinear equations but there are still some shortcomings, one is that improper initial values cause the interval solutions to be non-convergent, another limitation is that the range of results are too conservative due to interval dependency [9], which means that the bounds of IPF solutions are too wide. Affine Arithmetic (AA) method due to the ability that alleviate the dependency is gradually and widely used in IPF as an improved method, and which is being studied by many scholars.

AA is a self-validated model that is designed to alleviate the dependency problem in interval computations [10]. An affine variable is represented by a linear combination of a central value and a series of noises rather than intervals. Vaccaro *et al* proposed a methodology based on AA to analyze IPF problem [11], whose solution bounds are better and narrower than those obtained by traditional methods. Since then, various improved methods based on AA have been proposed and applied into power systems [12]–[15], i.e., a range arithmetic-based optimization model [12], the mixing method under rectangular and polar coordinate system [13], the method based on multi-stage AA [14] and the method based on evidence theory and AA [15]. In addition to IA and AA, many other algorithms and works are explored for improving IPF. Both the optimality-based bounds tightening (OBBT) method in [16] and moment-SOS approach in [17] are applied into IPF analysis to improve the accuracy of interval results. Moreover, a review of IPF calculation methods of power system in recent years has been made in [18]. For above references, the correlations among input random variables are not considered, and there is very little discussion of interval correlations for IPF problems in existing works.

Renewable energy sources and random loads, including wind turbines, photovoltaic generations and electric vehicles, *et al*, are constantly integrated into the distribution system. When distributed generations (DGs) and random loads are connected to the distribution system, the input data, just like bus injected power is not only intermittent and fluctuating, but also may be correlated to each other. In [19]–[22], Jiang *et al.* described the correlated and independent interval variables in a unified framework. At first, a new multidimensional ellipsoid model is described in [19], which can be regarded as a fundamental tool to relieve the correlations among variables. Afterwards, multidimensional parallelepiped (MP) convex model is proposed in [20]–[22], and this model is compared with the interval model and ellipsoid model. The comparative results show that MP model is more concise and more precise, so interval solutions can be obtained by using MP model. In this paper, a two-dimensional parallelepiped model, that is parallelogram model (PM), is applied to IPF problems in distribution power system based on AA theory, and the improvements made are as follows:

(1) For the distribution system integrated with DGs and loads, not only the strong randomness exists in DGs and loads with sources, but also the correlations are in them [23], [24]. The correlations of input variables (DGs-DGs and DGs-loads) in PF calculation are what this paper needs to consider, which can reduce the conservatism of IPF.

(2) The method that calculates the IPF solutions based on AA in [11] actually transforms the iterative process into a nonlinear optimization problem, yet the interval correlations mentioned above are not considered until now. In fact, nonlinear optimization is composed by objective functions and a series of constraints. The PM model is used to build new constraints obtained by the correlations of input variables (DGs-DGs and DGs-loads), which enhance overall constraints in optimization problem. Accordingly, the interval solutions of IPF are more accurate because of new constraints with correlations.

(3) The influence of the uncertainty level and different correlations of input variables on IPF are analyzed in this paper. Uncertainty level can be expressed by the fluctuation tolerance, which determines the shape and size of PM model. Correspondingly, the constraints are also affected by fluctuation tolerance. Another, the different correlations of input variables are divided into DGs-DGs and DGs-loads, which both have impacts on the IPF.

The rest of this paper is organized as follows: Section II introduces interval correlation model, including traditional IA method and PM model. Section III states a brief review of the IPF based on AA. In Section IV, the method using PM to IPF is analyzed. To verify the effectiveness of proposed

method and explore the influence of uncertainty level and the different correlations of input variables on IPF, numerical cases and three distribution system cases, i.e., IEEE33-bus, PG&E69-bus and IEEE118-bus distribution power system, are discussed in Section V. Finally, conclusions of this paper are summarized in Section VI.

II. INTERVAL CORRELATION MODEL

A. THE FUNDAMENTALS OF INTERVAL ARITHMETIC

IA is an attractive method to solve uncertainty problem because it can reduce the impact of objective factors and improve the reliability of analysis results. IA is a convenient algorithm proposed by Moore in 1979 [4], and he also defined interval variables and interval basic operations.

An interval number $[\underline{x}, \overline{x}]$ is the set of real numbers x such that $\underline{x} \le x \le \overline{x}$. Then a closed interval x is defined as:

$$x = [\underline{x}, \bar{x}] = \left\{ x \in \mathbf{R} \,\middle|\, \underline{x} \le x \le \bar{x} \right\} \tag{1}$$

where $\underline{x}, \overline{x}$ are elements of set $\mathbf{R}$ and are the lower and upper bounds of the interval variable x, respectively.

For two interval variables x and y, the addition, subtraction, multiplication, and division are defined in [4]. IA operations play an important role in uncertain analysis for so many years. However, overestimation problem always exits in traditional IA operations due to a dependency assumption [10]. That is to say, although IA can describe the variation range of the uncertainty, it cannot express the correlation among interval variables. For example, interval variable $x = [-1, 1]$, it minus itself get $x - x = \left[\underline{x} - \overline{x}, \overline{x} - \underline{x}\right] = [-2, 2]$ by the current IA operations rather than the exact result [0, 0]. The reason for this ''illness'' is that the correlations for input variables aren't considered according to [21].

B. PARALLELOGRAM MODEL

A two-dimensional PM is developed by Professor C. Jiang, who took into account independent and dependent interval variables in a unified framework [21]. For the PM, the given samples of variable space should be enclosed by establishing a parallelogram, and the parallelogram with a minimum area is considered as the best one. The correlations of interval variables and variation ranges are reflected by the position and size of specific parallelogram.

Fig. 1 is taken as an example to explain how the PM cures the ''illness'' that traditional IA usually overestimates the interval calculation results.

For Fig.1, x_1^c, x_2^c and x_1^w, x_2^w are the midpoints and radiuses of interval variables x_1, x_2, respectively.

$$\begin{aligned} x^c &= (\bar{x} + \underline{x})/2, \\ x^w &= (\bar{x} - \underline{x})/2. \end{aligned} \tag{2}$$

It is easy to know that the interval variables x_1 and x_2 are composed by the rectangle $ABCD$ in Fig. 1 as the correlation is not considered. However, the samples may not fill the entire rectangle $ABCD$ when there is correlation between x_1 and x_2. Parallelogram $AECF$ is more suitable for describing

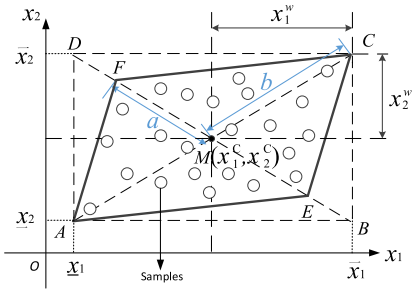

FIGURE 1. The parallelogram model.

x_1 and x_2 in this case, that is PM. In this model, the correlation coefficient $\rho_{x_1x_2}$ between variables x_1 and x_2 is defined as follows:

$$\rho_{x_1x_2} = \frac{b - a}{b + a} \tag{3}$$

where a and b denote the semi-diagonal length of the parallelogram in the direction of MF and MC.

The explicit expression of PM is described in (4) shown in reference [3]:

$$\left| \boldsymbol{\rho}^{-1} \boldsymbol{T}^{-1} \boldsymbol{R}^{-1} (\boldsymbol{x} - \boldsymbol{x}^c) \right| \le e \tag{4}$$

where $|\cdot|$ denotes the absolute value in it, and the matrices $\boldsymbol{\rho}$, $\boldsymbol{T}$, $\boldsymbol{R}$, $\boldsymbol{x}$, $\boldsymbol{x^c}$ and $\boldsymbol{e}$ are defined as:

$$\begin{aligned} \boldsymbol{\rho} &= \begin{bmatrix} \rho_{x_1x_1} & \rho_{x_1x_2} \\ \rho_{x_2x_1} & \rho_{x_2x_2} \end{bmatrix} = \begin{bmatrix} 1 & \rho_{12} \\ \rho_{21} & 1 \end{bmatrix} \\ \boldsymbol{T} &= \begin{bmatrix} w_1 & 0 \\ 0 & w_2 \end{bmatrix} \quad w_i = \frac{1}{\sum_{j=1}^{2} \left| \rho_{ij} \right|}, \\ \boldsymbol{R} &= \begin{bmatrix} x_1^w & 0 \\ 0 & x_2^w \end{bmatrix} \\ \boldsymbol{x} &= \begin{bmatrix} x_1 \\ x_2 \end{bmatrix} \boldsymbol{x}^c = \begin{bmatrix} x_1^c \\ x_2^c \end{bmatrix} \quad \boldsymbol{e} = [-1, 1]^T \end{aligned} \tag{5}$$

It is assumed that vector $\boldsymbol{\delta} = [\delta_1 \delta_2]^{\mathrm{T}}$ and $\delta_i = [-1, 1]$ $(i = 1, 2)$, then standard expression of two correlated interval variables can be obtained from (4):

$$\boldsymbol{x} = \boldsymbol{RT\rho\delta} + \boldsymbol{x}^c \tag{6}$$

According to the PM and the standard expression in (4), correlated interval variables are converted into independent ones [21], whose specific steps and examples are described in Section V.

As for N interval random variables, i.e., DGs, random loads in power system, the correlation coefficient matrix $\boldsymbol{\rho}$ can be described as

$$\boldsymbol{\rho} = \begin{bmatrix} \rho_{11} & \rho_{12} & \cdots & \rho_{1N} \\ \rho_{21} & \rho_{22} & \cdots & \rho_{2N} \\ \vdots & \vdots & \ddots & \vdots \\ \rho_{N1} & \rho_{N2} & \cdots & \rho_{NN} \end{bmatrix} = \begin{bmatrix} 1 & \rho_{12} & \cdots & \rho_{1N} \\ \rho_{21} & 1 & \cdots & \rho_{2N} \\ \vdots & \vdots & \ddots & \vdots \\ \rho_{N1} & \rho_{N2} & \cdots & 1 \end{bmatrix} \tag{7}$$

where $\boldsymbol{\rho}$ is an $N \times N$ symmetric correlation matrix, and the $\boldsymbol{e}$ is $N \times 1$ vector.

The uncertain domain for the N interval variables can be described as

$$\left|\boldsymbol{\rho}^{-1}\boldsymbol{T}^{-1}\boldsymbol{R}^{-1}\begin{pmatrix} X_1 - X_1^C \\ \vdots \\ X_N - X_N^C \end{pmatrix}\right| = \left|\boldsymbol{C}^{-1}\begin{pmatrix} X_1 - X_1^C \\ \vdots \\ X_N - X_N^C \end{pmatrix}\right| \leq \boldsymbol{e} \tag{8}$$

where the matrices $\boldsymbol{T}$, $\boldsymbol{R}$, $\boldsymbol{C}$ are the $N \times N$ matrix.

III. INTERVAL POWER ANALYSIS BASED ON AA

PF calculation is the most basic and important tool of power system analysis. However, large-scale uncertain loads demand and generator power output accessed to power system make it difficult to obtain the solutions of uncertain power flow with traditional PF calculation method. IA method is used to deal with uncertain problem for IPF, that is, only approximate range of solution is needed instead of exact value information. We know that there are conservative defects when IA is applied to functions according to Section II, so the AA is utilized in this paper.

A. AFFINE ARITHMETIC

AA is proposed to overcome the shortcomings of IA. In terms of AA, an interval variable $x = [\underline{x}, \overline{x}]$ is expressed as the combination of a central value x_0 and noises $x_i\varepsilon_i$ as

$$x = x_0 + x_1\varepsilon_1 + x_2\varepsilon_2 + \cdots + x_n\varepsilon_n \tag{9}$$

where $\varepsilon_i (i = 1, 2, \ldots, n)$ is noise symbol and $x_i (i = 1, 2, \ldots, n)$ is associated coefficient. The specific value of each noise is unknown except that it is restricted to $\varepsilon_i = [-1, 1] (i = 1, 2, \ldots, n)$ and each noise is independent from the other noise symbols.

AA and IA can be transformed each other. An affine form variable x can be expressed as $x = [x_0 - r, x_0 + r]$, and the radius r can be computed as $r = \sum_{i=1}^{n} |x_i|$, where r is called the total deviation for x. Conversely, an interval variable $x = [a, b]$ can be switched affine form as $x = x_0 + x_i\varepsilon_i$, where $x_0 = (b + a)/2$ and $x_i = (b - a)/2$. There is more additional relevant information in affine form, so the solutions are more accurate by using AA.

Key feature of AA is that different affine form variables may have some same noise symbols. Thus, given two affine form variables x and y:

$$x = x_0 + x_1\varepsilon_1 + x_2\varepsilon_2 + \cdots + x_n\varepsilon_n$$
$$y = y_0 + y_1\varepsilon_1 + y_2\varepsilon_2 + \cdots + y_n\varepsilon_n$$

The basic operations of affine form are defined as:

$$\alpha x + \beta y + \gamma = (\alpha x_0 + \beta y_0 + \gamma) + (\alpha x_1 + \beta y_1)\varepsilon_1 + \cdots + (\alpha x_n + \beta y_n)\varepsilon_n \tag{10}$$

where α, β and γ are three real numbers,

$$\begin{aligned} x \cdot y &= (x_0 + \sum_{i=1}^{n} x_i\varepsilon_i) \cdot (y_0 + \sum_{i=1}^{n} y_i\varepsilon_i) \\ &= x_0y_0 + \sum_{i=1}^{n}(x_0y_i + y_0x_i)\varepsilon_i + \sum_{i=1}^{n} x_i\varepsilon_i \cdot \sum_{i=1}^{n} y_i\varepsilon_i \\ &= x_0y_0 + \sum_{i=1}^{n}(x_0y_i + y_0x_i)\varepsilon_i + z_k\varepsilon_k \end{aligned} \tag{11}$$

where ε_k is the new noise and z_k is the new coefficient that can be calculated by $z_k = \sum_{i=1}^{n} |x_i| \cdot \sum_{i=1}^{n} |y_i|$. In the same way, we can get x/y through $x \cdot (1/y)$.

B. INTERVAL POWER FLOW

Firstly, typical PF equations under rectangular coordinate system are

$$\begin{cases} P_i = e_i \sum_{j=1}^{n}(G_{ij}e_j - B_{ij}f_j) + f_i \sum_{j=1}^{n}(G_{ij}f_j + B_{ij}e_j) \\ Q_i = f_i \sum_{j=1}^{n}(G_{ij}e_j - B_{ij}f_j) - e_i \sum_{j=1}^{n}(G_{ij}f_j + B_{ij}e_j) \\ \quad \forall i \in n_{PQ} \end{cases} \tag{12}$$

and

$$\begin{cases} P_i = e_i \sum_{j=1}^{n}(G_{ij}e_j - B_{ij}f_j) + f_i \sum_{j=1}^{n}(G_{ij}f_j + B_{ij}e_j) \\ V_i^2 = e_i^2 + f_i^2 \quad \forall i \in n_{PV} \end{cases} \tag{13}$$

where

n	system total bus number;
n_{PQ}	list of PQ-bus;
n_{PV}	list of PV-bus;
$G_{ij} + jB_{ij}$	G_{ij}, B_{ij} are real and imaginary part of Y_{ij} respectively, where Y_{ij} is the bus admittance matrix;
$e_i + jf_i$	e_i, f_i are real and imaginary part of V_i, where $\sqrt{e_i^2 + f_i^2} = V_i$ is the ith bus voltage magnitude;
$\theta_{ij} = \theta_i - \theta_j$	θ_i, θ_j are angles of V_i, V_j respectively.

For IPF, the injected active power P_i and reactive power Q_i are regarded as intervals just like $[P_i^{\min}, P_i^{\max}]$ and $[Q_i^{\min}, Q_i^{\max}]$ because of uncertain loads and renewable energy generations, and then the power flow solutions, i.e., bus voltage magnitude, voltage angle and the line flows, are also intervals. In other words, these input power variations lead to the fluctuations for solutions of PF results. Therefore, we assume that ε_i^P, ε_i^Q are injected active and reactive power noises at the ith bus respectively, and their initial values are both $[-1, 1]$. According to reference [11], the state variables of power system in rectangular coordinates are described as affine form:

$$\begin{cases} e_i = e_{i,0} + \sum_{j \in nP} e_{ij}^P \varepsilon_j^P + \sum_{j \in n_{PQ}} e_{ij}^Q \varepsilon_j^Q \\ f_i = f_{i,0} + \sum_{j \in nP} f_{ij}^P \varepsilon_j^P + \sum_{j \in n_{PQ}} f_{ij}^Q \varepsilon_j^Q \quad i \in nP \end{cases} \tag{14}$$

where

nP	list of PQ-bus and PV-bus;
$e_{i,0}, f_{i,0}$	central value of e_i and f_i;
e_{ij}^P, f_{ij}^P	partial deviation of e_i and f_i due to the active power injected at the jth bus;
e_{ij}^Q, f_{ij}^Q	partial deviation of e_i and f_i due to the reactive power injected at the jth bus;

Parameters in (14) $e_{i,0}, f_{i,0}, e_{ij}^P, f_{ij}^P, e_{ij}^Q, f_{ij}^Q$ are all unknown but can be calculated by the formulations in [13], whose specific calculation expressions are as follows:

$$\begin{aligned} e_{ij}^P &= \left.\frac{\partial e_i}{\partial P_j}\right|_0 \Delta P_j, \quad f_{ij}^P = \left.\frac{\partial f_i}{\partial P_j}\right|_0 \Delta P_j \\ e_{ij}^Q &= \left.\frac{\partial e_i}{\partial Q_k}\right|_0 \Delta Q_k, \quad f_{ij}^Q = \left.\frac{\partial f_i}{\partial Q_k}\right|_0 \Delta Q_k \\ &\qquad for\ i, j \in n\ Pk \in nQ \end{aligned} \tag{15}$$

where these partial derivatives $\frac{\partial e_i}{\partial P_j}|_0$, $\frac{\partial f_i}{\partial P_j}|_0$, $\frac{\partial e_i}{\partial Q_k}|_0$, $\frac{\partial f_i}{\partial Q_k}|_0$ can be obtained by the inverse of the Jacobi matrix for deterministic PF at point $e_{i,0}$ and $f_{i,0}$. As for $e_{i,0}$ and $f_{i,0}$, they can be obtained by deterministic PF or MC as the central value references. ΔP_j and ΔQ_k represent the radii of interval $[P_j^{\min}, P_j^{\max}]$ and $[Q_k^{\min}, Q_k^{\max}]$ respectively. That is, $\Delta P_j = (P_j^{\max} - P_j^{\min})/2$ and $\Delta Q_k = (Q_k^{\max} - Q_k^{\min})/2$.

Then we replace e_i and f_i in (12) and (13) with the affine form in (14). After basic operations by AA, the following AA form of injected powers can be obtained:

$$\begin{cases} P_i = P_{i,0} + \sum_{j\in nP} P_{ij}^P \varepsilon_j^P + \sum_{j\in nQ} P_{ij}^Q \varepsilon_j^Q + \sum_{k\in nN} P_{ik}\varepsilon_k \\ Q_i = Q_{i,0} + \sum_{j\in nP} Q_{ij}^P \varepsilon_j^P + \sum_{j\in nQ} Q_{ij}^Q \varepsilon_j^Q + \sum_{k\in nN} Q_{ik}\varepsilon_k \\ \qquad \forall i \in PQ \end{cases} \tag{16}$$

and

$$\begin{cases} P_i = P_{i,0} + \sum_{j\in nP} P_{ij}^P \varepsilon_j^P + \sum_{j\in nQ} P_{ij}^Q \varepsilon_j^Q + \sum_{k\in nN} P_{ik}\varepsilon_k \\ V_i^2 = V_{i,0}^2 + \sum_{j\in nP} V_{ij}^P \varepsilon_j^P + \sum_{j\in nV} V_{ij}^Q \varepsilon_j^Q + \sum_{k\in nN} V_{ik}\varepsilon_k \\ \qquad \forall i \in PV \end{cases} \tag{17}$$

where

$P_{i,0}$	central value of interval active power, which is $(P_i^{min} + P_i^{max})/2$;
$Q_{i,0}$	central value of interval reactive power, which is $(Q_i^{min} + Q_i^{max})/2$;
$V_{i,0}^2$	known value of PV-bus;
ε_k	new noises generated during the calculation;

$P_{ij}^P, P_{ij}^Q, P_{ik}, Q_{ij}^P, Q_{ij}^Q, Q_{ik}, V_{ij}^P, V_{ij}^Q, V_{ik}$ new coefficients of noises ε_j^P, ε_j^Q and ε_k.

Generally, it is assumed that subscripts $1, 2, \ldots, m$ denote PQ buses, subscripts $m+1, m+2, \ldots, n-1$ denote PV buses and subscript n denotes the slack bus. The affine forms (16) and (17) can be converted into the matrix form in (18), as shown at the bottom of this page.

$$\begin{bmatrix} [P_1^{\min}, P_1^{\max}] \\ \vdots \\ [P_{n-1}^{\min}, P_{n-1}^{\max}] \\ [Q_1^{\min}, Q_1^{\max}] \\ \vdots \\ [Q_m^{\min}, Q_m^{\max}] \\ [V_{m+1}^2, V_{m+1}^2] \\ \vdots \\ [V_{n-1}^2, V_{n-1}^2] \end{bmatrix} = \begin{bmatrix} P_{1,0} \\ \vdots \\ P_{n-1,0} \\ Q_{1,0} \\ \vdots \\ Q_{m,0} \\ V_{m+1,0}^2 \\ \vdots \\ V_{n-1,0}^2 \end{bmatrix} + \begin{bmatrix} P_{11}^P & P_{12}^P & \cdots & P_{1,n-1}^P & P_{11}^Q & P_{12}^Q & \cdots & P_{1,m}^Q \\ \vdots & \vdots & \vdots & \vdots & \vdots & \vdots & \vdots & \vdots \\ P_{n-1,1}^P & P_{n-1,2}^P & \cdots & P_{n-1,n-1}^P & P_{n-1,1}^Q & P_{n-1,2}^Q & \cdots & P_{n-1,m}^Q \\ Q_{11}^P & Q_{12}^P & \cdots & Q_{1,n-1}^P & Q_{11}^Q & Q_{12}^Q & \cdots & Q_{1,m}^Q \\ \vdots & \vdots & \vdots & \vdots & \vdots & \vdots & \vdots & \vdots \\ Q_{m,1}^P & Q_{m,2}^P & \cdots & Q_{m,n-1}^P & Q_{m,1}^Q & Q_{m,2}^Q & \cdots & Q_{m,m}^Q \\ V_{m+1,1}^P & V_{m+1,2}^P & \cdots & V_{m+1,n-1}^P & V_{m+1,1}^Q & V_{m+1,2}^Q & \cdots & V_{m+1,m}^Q \\ \vdots & \vdots & \vdots & \vdots & \vdots & \vdots & \vdots & \vdots \\ V_{n-1,1}^P & V_{n-1,2}^P & \cdots & V_{n-1,n-1}^P & V_{n-1,1}^Q & V_{n-1,2}^Q & \cdots & V_{n-1,m}^Q \end{bmatrix} \cdot \begin{bmatrix} \varepsilon_1^P \\ \varepsilon_2^P \\ \vdots \\ \varepsilon_{n-1}^P \\ \varepsilon_1^Q \\ \varepsilon_2^Q \\ \vdots \\ \varepsilon_m^Q \end{bmatrix} + \begin{bmatrix} P_{11} & P_{12} & \cdots & P_{1,nN} \\ \vdots & \vdots & \cdots & \vdots \\ P_{n-1,1} & P_{n-1,2} & \cdots & P_{n-1,nN} \\ Q_{11} & Q_{12} & \cdots & Q_{1,nN} \\ \vdots & \vdots & \vdots & \vdots \\ Q_{m,1} & Q_{m,2} & \cdots & Q_{m,nN} \\ V_{m+1,1} & V_{m+1,2} & \cdots & V_{m+1,nN} \\ \vdots & \vdots & \vdots & \vdots \\ V_{n-1,1} & V_{n-1,2} & \cdots & V_{n-1,nN} \end{bmatrix} \begin{bmatrix} \varepsilon_1 \\ \varepsilon_2 \\ \vdots \\ \varepsilon_{nN} \end{bmatrix} \tag{18}$$

Correspondingly, the more general form can be written as

$$f = C + AX + BY \tag{19}$$

where

$$f = \left[\left[P_1^{\min}, P_1^{\max}\right] \quad \cdots \quad \left[V_{n-1}^2, V_{n-1}^2\right]\right]^T,$$
$$C = \left[P_{1,0} \quad \cdots \quad V_{n-1,0}^2\right]^T,$$
$$A = \begin{bmatrix} P_{11}^P & \cdots & P_{1,m}^Q \\ \vdots & \ddots & \vdots \\ V_{n-1,1}^P & \cdots & V_{n-1,m}^Q \end{bmatrix},$$
$$B = \begin{bmatrix} P_{11} & \cdots & P_{1,nN} \\ \vdots & \ddots & \vdots \\ V_{n-1,1} & \cdots & V_{n-1,nN} \end{bmatrix}$$
$$X = [\varepsilon_1^P \varepsilon_2^P \cdots \varepsilon_{n-1}^P \varepsilon_1^Q \varepsilon_1^Q \cdots \varepsilon_m^Q]^T,$$
$$Y = [\varepsilon_1 \varepsilon_2 \cdots \varepsilon_{nN}]^T.$$

As discussed in [11] and [13], the range of IPF can be reduced by contracting variable X, while Y cannot be contracted. Because X is the original noises we assumed, but Y is the new noises generated by the calculation process. That means the elements in X will become narrower than $[-1, 1]$ after calculation and the elements for Y have always remained the same $[-1, 1]$. Actually, the IPF problem is changed into nonlinear optimization problem about noises ε_i according to [11] and [13], where (19) denotes constraint conditions and the PF solutions of affine form to be solved can be treated as the objective functions. From [13], we know that one of the constraints can be obtained by (19) and expressed as

$$AX = f - C - BY = D = [\inf(D), \sup(D)] \tag{20}$$

According to the definition of ε_i and (20), the constraints about ε_i can be also expressed as (21):

$$s.t. \begin{cases} -1 \le \varepsilon_i^P \le 1, \quad i = 1, 2, \ldots, n-1 \\ -1 \le \varepsilon_i^Q \le 1, \quad i = 1, 2, \ldots, m \\ \inf(D_i) \le (AX)_i = \sum_{j=1}^{n-1} A_{ij}\varepsilon_j^P + \sum_{j=1}^{m} A_{ij}\varepsilon_j^Q \le \sup(D_i), \\ \quad i = 1, 2, \ldots, 2n-2 \end{cases} \tag{21}$$

where D can be obtained by calculating (20), and the D_i, $(AX)_i$ represent the ith element of D and AX respectively.

As we all know, the solutions of PF are bus voltage magnitude V_i, bus voltage angle θ_i, active power of branches P_{ij} and reactive power of branches Q_{ij}. In rectangular coordinate system, they can all be represented by these functions about e_i and f_i as shown in (22)-(25).

1) Voltage magnitude V_i

$$V_i^2 = e_i^2 + f_i^2 = (e_{i,0} + \sum_{j\in nP} e_{ij}^P \varepsilon_j^P + \sum_{j\in nQ} e_{ij}^Q \varepsilon_j^Q)^2 + (f_{i,0} + \sum_{j\in nP} f_{ij}^P \varepsilon_j^P + \sum_{j\in nQ} f_{ij}^Q \varepsilon_j^Q)^2 \tag{22}$$

2) Voltage angle θ_i

$$\theta_i = \arctan(f_i/e_i) = \arctan[(f_{i,0} + \sum_{j\in nP} f_{ij}^P \varepsilon_j^P + \sum_{j\in nQ} f_{ij}^Q \varepsilon_j^Q) / (e_{i,0} + \sum_{j\in nP} e_{ij}^P \varepsilon_j^P + \sum_{j\in nQ} e_{ij}^Q \varepsilon_j^Q)] \tag{23}$$

3) Active power of branches P_{ij}

$$P_{ij} = G_{ij}(e_i^2 + f_i^2 - e_i e_j - f_i f_j) + B_{ij}(e_i f_j - e_j f_i) \tag{24}$$

4) Reactive power of branches Q_{ij}

$$Q_{ij} = G_{ij}(e_i f_j - e_j f_i) - B_{ij}(e_i^2 + f_i^2 - e_i e_j - f_i f_j) \tag{25}$$

As can be seen from (22), (23), (24) and (25), these functions can all be converted into polynomials about noises ε_i. So the range of these solutions can be obtained by nonlinear optimization, that is, their min and max values can be obtained when (22)-(25) are as objective functions and (21) is as the constraints.

In summary, IPF solutions can be obtained by nonlinear optimization about noises ε_i, and the IPF solutions obtained by AA are better than that obtained by IA. But as mentioned in Section I, the correlations among some interval variables are not considered, the interval solutions are still not accurate enough. Naturally, the bounds of IPF solutions with interval correlations are becoming much narrower than those without correlations.

IV. INTERVAL POWER FLOW WITH CORRELATION

Section III describes the process of IPF calculation by AA. As discussed in Section I, it exists correlations for DGs-DGs and DGs-loads in distribution system. It is assumed that DGs-DGs and DGs-loads are accessed the ith and the jth bus in distribution system, and they have a certain correlations, then the correlations can be added as new constraints in (21).

Similarly, in (19), f, B, Y and C are known, and only X in AX is unknown. The intervals $[\inf(D_i),\sup(D_i)]$ can be obtained by calculating the known equation $f - C - BY = D$, and the uncertain AX is in these intervals D_i, which can be used as constraints about ε_i^P and ε_i^Q. Generally, the X can be well constrained by the upper and lower bounds of D_i, just as described in [13]. But D_i is not the optimal constraint of X, the reason is that it may exist correlations among the elements in f.

Next, the ith and the jth buses are used for analysis. Both $(AX)_i$ and $(AX)_j$ have upper and lower limits, which are expressed as

$$\begin{cases} \inf(D_i) \le (AX)_i \le \sup(D_i) \\ \inf(D_j) \le (AX)_j \le \sup(D_j) \end{cases} \tag{26}$$

These two inequalities in (26) are actually parts of $(2n-2)$ inequality constraints in formula (21), which are the ith and the jth respectively.

The inequalities in (26) presented as four lines AB, BC, CD and DA to form a rectangle ABCD in Fig. 2. But when

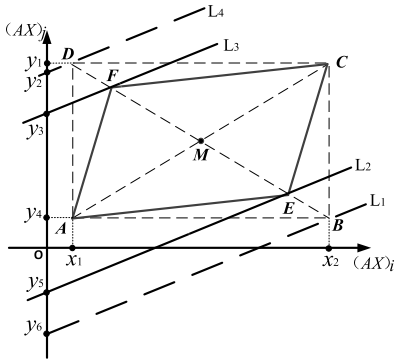

FIGURE 2. The constraint model with correlation.

considering the correlations of interval variables, the range of $(AX)_i$ and $(AX)_j$ should be described by a parallelogram $AECF$ instead of the rectangle $ABCD$ in Fig. 2.

where

Points: $x_1 = \inf(D_i), x_2 = \sup(D_i), y_1 = \sup(D_j), y_2 = \sup(kD_i + D_j), y_3 = \sup(D_{ij}), y_4 = \inf(D_j), y_5 = \inf(D_{ij}), y_6 = \inf(kD_i + D_j)$.

Line L_1: $(AX)_j = k(AX)_i + b$.

Actually, the area or size of parallelogram is narrowed compared to rectangle $ABCD$, which means the constraints are enhanced, so the parallelogram surrounded by four lines AE, EC, CF and FA are the optimal constraints. Now the problem is how to obtain the inequality constraints about these lines.

Firstly, a line can be expressed as $(AX)_j = k(AX)_i + b$ in Fig.2, which is equivalent to

$$b = (AX)_j - k(AX)_i \tag{27}$$

where $(AX)_i$ and $(AX)_j$ are intervals.

As for (27), b can be calculated as $b = [\inf(kD_i + D_j), \sup(kD_i + D_j)]$ by traditional IA method, which does not reduce the constraint area as shown by the lines L_1 and L_4 in Fig.2. Through PM method mentioned in Section II, b can be calculated as $b = [\inf(D_{ij}), \sup(D_{ij})]$, which the constraint area is reduced as shown by the lines L_2 and L_3.

That is to say, regardless of the slope k, the constraints cannot be enhanced by IA method. But as long as the slope k is appropriate, the constraints can be optimal by the PM method. The optimal slope k can be obtained by the borderlines of PM. So the improved constraints are

$$s.t. \begin{cases} -1 \le \varepsilon_i^P \le 1, \quad i = 1, 2, \ldots, n-1 \\ -1 \le \varepsilon_i^Q \le 1, \quad i = 1, 2, \ldots, m \\ \inf(D_i) \le (AX)_i = \sum_{j=1}^{n-1} A_{ij}\varepsilon_j^P + \sum_{j=1}^{m} A_{ij}\varepsilon_j^Q \le \sup(D_i), \\ \qquad i = 1, 2, \ldots, 2n-2 \\ \inf(D_{ij}) \le k(AX)_i + (AX)_j \le \sup(D_{ij}), \\ \qquad i, j \in 1, 2, \ldots, 2n-2 \end{cases} \tag{28}$$

where $D_{ij} = [\inf(D_{ij}), \sup(D_{ij})]$ is calculated by PM method.

In a word, new constraints are described as the following two cases:

1) without correlation

$$\inf(kD_i + D_j) \le k(AX)_i + (AX)_j \le \sup(kD_i + D_j) \tag{29}$$

In this case, (29) is same as (26), that is, $D_{ij} = kD_i + D_j$.

2) with correlation

According to the description above, it exists that $D_{ij} \subseteq kD_i + D_j$ as the correlations of input variables is considered, original constraints are enhanced by adding new constraints. The bounds of IPF solutions are tighter.

Generally speaking, the flow chart of the proposed method is shown in Fig. 3 and the process of the proposed method is illustrated according to following steps.

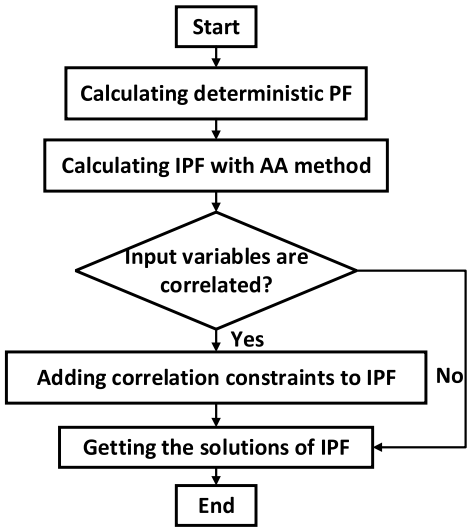

FIGURE 3. Process of the proposed method.

Step 1: Writing the typical PF equations under rectangular coordinate system presented in (12), (13) and obtaining the solutions of deterministic PF.

Step 2: The output power of DGs and random loads are regarded as the source of interval fluctuation. The affine form of PF equations in (18) is obtained by assuming ε_i^P and ε_i^Q represent the injected active and reactive power noises at the ith bus respectively.

Step 3: The affine form of PF equations in (18) is written as the constraints in (21) about noises ε_i, which includes the boundary of noises ε_i $[-1, 1]$ and the boundary of $(AX)_i$ obtained by transforming (18).

Step 4: The correlations of input variables (DGs-DGs and DGs-loads) are transformed into the constraints through PM model. The constraints (28) can be obtained by integrating the additional correlations constraint into (21).

Step 5: The objective functions (22)-(25), i.e., the affine form of bus voltage magnitude, voltage angle, active and reactive power of branches, are obtained. Interval solutions of IPF problem combing with objective functions (22)-(25) and constraints (28) can be obtained through optimization algorithm such as the fmincon of Matlab.

V. CASE STUDY

In this section, a numerical case and three case studies about distribution system are discussed. In the first numerical case, it is used to prove that the interval solution does become more accurate with considering the correlations of input variables. In the second case, the correctness and effectiveness of the proposed method are proved with IEEE33-bus distribution system. In the third case, we test the effects of different injected power uncertainty levels on the IPF with PG&E69-bus distribution system. The results show that the widths of IPF solutions are much tighter with the interval correlations, and the final interval solutions are also affected by uncertainty level. In the last case, the IEEE118-bus distribution system illustrates the optimization level as a supplementary example.

A. NUMERICAL CASE

Two interval variables $x_1 = [2, 4]$ and $x_2 = [2, 4]$ are considered in this case, which are calculated by traditional IA and the proposed method.

Taking the function $f = x_1 + x_2$ as an example. It is assumed that the correlation coefficient between x_1 and x_2 is $\rho = -0.2$ (The positive correlation is not considered due to similarity), then the following expression (30) can be obtained according to (6):

$$\begin{aligned}\begin{bmatrix} x_1 \\ x_2 \end{bmatrix} &= \boldsymbol{RT\rho\delta} + \boldsymbol{x}^c \\ &= \begin{bmatrix} 1 & 0 \\ 0 & 1 \end{bmatrix}\begin{bmatrix} 1/1.2 & 0 \\ 0 & 1/1.2 \end{bmatrix} \\ &\quad \times \begin{bmatrix} 1 & -0.2 \\ -0.2 & 1 \end{bmatrix}\begin{bmatrix} \delta_1 \\ \delta_2 \end{bmatrix} + \begin{bmatrix} 3 \\ 3 \end{bmatrix} \end{aligned} \tag{30}$$

In this way, the function $f(x)$ with correlations is transformed into the function $f(\delta)$ with only independent variables.

$$\begin{aligned} f(\delta) &= (0.8333\delta_1 - 1.6667\delta_2 + 3) \\ &\quad + (-1.6667\delta_1 + 0.8883\delta_2 + 3) \\ &= [4.6668, 7.3332] \end{aligned} \tag{31}$$

Compared the interval result [4, 8] using traditional IA with the interval result [4.6691, 7.3296] using Monte Carlo (MC), it can be seen that the interval results obtained by the proposed method are really much narrower.

Of course, one example does not lead to the general conclusion, so some different correlation coefficients ρ and different objective functions $f(x)$ are analysed. The objective functions are as follows:

$$\begin{aligned} f_1 &= x_1 + x_2 \\ f_2 &= x_1 \cdot x_2 - x_1 + x_2 \\ f_3 &= x_1^2 - x_2^2 - x_1 \cdot x_2 + x_1 + x_2 \end{aligned}$$

The sample size of MC is set to 10,000, which is treated as the true value. The results are shown in Table 1.

For the function f_1, the interval results obtained from MC and the method with & without correlation are all [4, 8] when correlation coefficient is set as 0.2. Compared to the interval result [4.669, 7.330] obtained by MC, the function interval value [4.667, 7.333] obtained by the method with correlation is closer than the interval result [4, 8] without correlation when the coefficient is set as -0.2. As for f_2 and f_3, their interval results are all affected by the correlations, whether the correlation coefficient is positive or negative. However, the degree of correlation influence is different. The proposed method is effective to solve these functions whose input variables are correlative.

TABLE 1. Comparison of results with and without correlation.

Functions	Coefficient	Without Correlation	With Correlation	Monte Carlo
f_1	0.2	[4,8]	[4,8]	[4,8]
	-0.2		[4.667,7.333]	[4.669,7.330]
f_2	0.4	[2,18]	[2.000,15.999]	[4.000,8.000]
	-0.4		[5.428,12.571]	[6.000,11.753]
f_3	0.6	[-24,16]	[-8.031,2.031]	[-8.000,0.068]
	-0.6		[-16.031,10.031]	[-13.999,10.00]

In order to reflect the universality of the proposed method, we can apply this method into the IPF problem with interval correlations in distribution power system.

B. IEEE33-BUS DISTRIBUTION SYSTEM

The single line diagram and load parameters of IEEE33-bus distribution system can be found in paper [25]. There are many ways to select parameters, i.e., the number, location and capacity of DGs and random loads such as electric vehicles, but just as an example, it is assumed that five DGs with 500+j150kVA and one additional load with 300+j100kVA are integrated into IEEE33-bus distribution system as shown in Fig.4. The correlations of bus 18 and 33 with DGs, bus 25 and 29 with DGs, bus 9 with DG and bus 10 with load are considered, and the fluctuation tolerance of output power of all DGs and loads is ±10%. The correlations for the DGs-DGs and DGs-loads are set as −0.8 in this paper (The positive correlation is not considered due to similarity). The results obtained by MC simulation with correlations are regarded as the 'true' bounds of IPF, and the sample number is set to 10,000 to ensure accurate level. For MC simulation, the samples of two interval variables are in parallelogram shown in Fig.1. The calculation results of IPF are presented in Fig.5, Fig.6 and Fig.7.

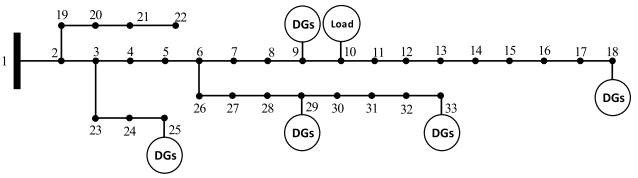

FIGURE 4. The single line diagram of IEEE33-bus system.

It can be observed that the deterministic PF is between upper and lower bounds of interval results obtained by three

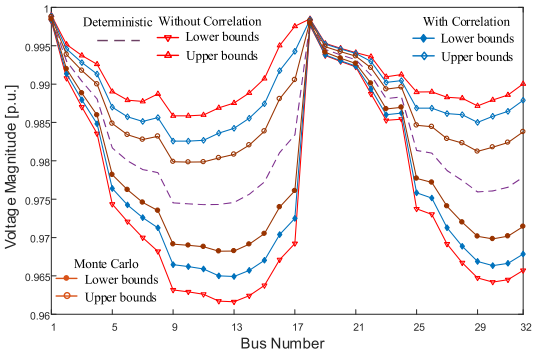

FIGURE 5. The results of bus voltage magnitude of IEEE33-bus system.

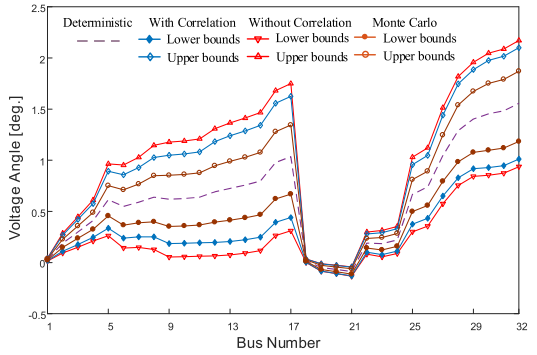

FIGURE 6. The results of bus voltage angle of IEEE33-bus system.

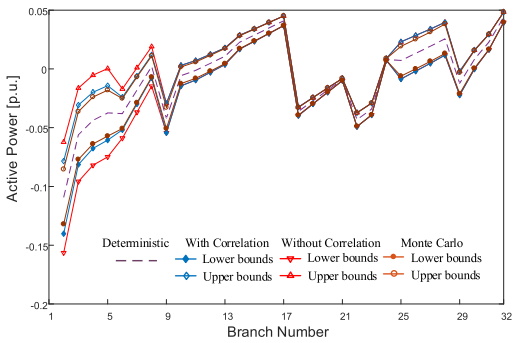

FIGURE 7. The results of active power of IEEE33-bus system.

different methods (with correlation, without correlation and MC) from Figs.5∼7. Compared to the interval bus voltage magnitude without correlation, the bounds with correlation are closer to the 'true' bounds of MC from Fig.5. Same to voltage magnitude, the bus voltage angle and active power of branches have the same optimized performance according to Fig.6 and Fig.7. It shows that the accuracy of the IPF solutions is improved when the correlation of input variables are considered. The reason is that the interval extension is emphasized by the method with correlation while is ignored by the method without correlation. In other words, the feasible region of IPF solutions is smaller as the correlation of input variables in proposed method are considered.

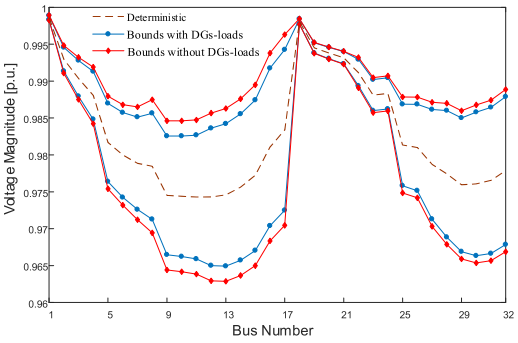

FIGURE 8. Impact of correlation with/without DGs-loads.

To research the influence of DGs-loads with correlations on IPF, the correlated buses considered are divided two situations: first one is the correlations of DGs-DGs (bus 18, 33) and DGs-DGs (bus 25, 29) are considered, another is the correlations of DGs-DGs (bus 18, 33), DGs-DGs (bus 25, 29) and DGs-loads (bus 9, 10) are considered. It is assumed that the fluctuation tolerance of output power for all DGs and loads is $\pm 10\%$, and the correlation coefficients are set as -0.8. Two different voltage magnitude of IPF are shown in Fig. 8. The bounds with correlations of DGs-loads are narrower than the ones without correlations of DGs-loads. The boundaries of IPF become narrower because the number of correlated buses considered increases, no matter whether the correlated buses are DGs or loads.

C. PG&E69-BUS DISTRIBUTION SYSTEM

The single line diagram and parameters of PG&E69-bus distribution system can be found in paper [26]. Similar to IEEE33-bus distribution system, it is assumed that five DGs (bus 15, 27, 39, 54, 69) with $1000+j300$kVA and one additional load (bus 48) with $800+j200$kVA are integrated into PG&E69-bus distribution system, and the correlations of bus 15 and 69, bus 27 and 54, bus 39 and 48 are considered. The fluctuation tolerance of output power of all generators and loads is $\pm 15\%$, the correlation coefficients for DGs-DGs and DGs-loads are set as -0.6 (The positive correlation is not considered due to similarity).

Firstly, we can get the same conclusion that the accuracy of the IPF solutions is narrowed when the correlations are considered from Figs.9∼11. However, compared with the results shown in Figs.5∼7, the interval widths of IPF solutions between "with correlation" and "without correlation" seem much smaller in PG&E69-bus distribution system than the interval widths obtained in IEEE33-bus distribution system. The important reason is that the scale of PG&E69-bus distribution system is larger than IEEE33-bus distribution system, but the number of DGs and additional loads integrated into network are also just six. The effect caused by the correlation becomes more obvious when the number of DGs increases.

TABLE 2. Comparison of results of evaluation indexes.

Systems	Without Correlation				With Correlation				MC(10,000)
	A_{max}	A_{min}	A	Time/s	A_{max}	A_{min}	A	Time/s	Time/s
IEEE33	57.25%	39.28%	46.45%	2.09	66.36%	50.27%	61.43%	3.09	17.84
PG&E69	90.55%	46.89%	63.73%	10.02	91.54%	65.28%	70.54%	11.66	71.87
IEEE118	84.78%	32.74%	56.38%	29.27	88.09%	34.15%	60.16%	32.49	199.55

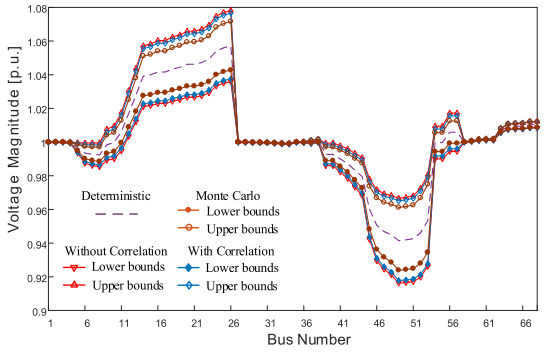

FIGURE 9. The results of bus voltage magnitude of PG&E69-bus system.

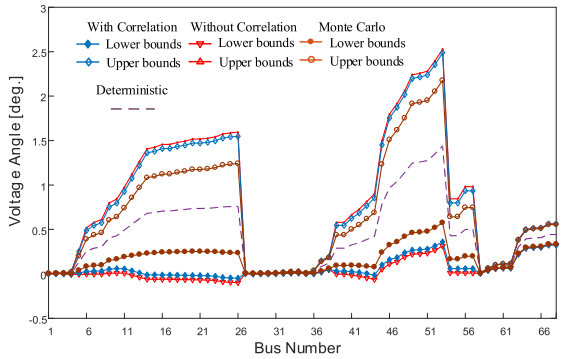

FIGURE 10. The results of bus voltage angle of PG&E69-bus system.

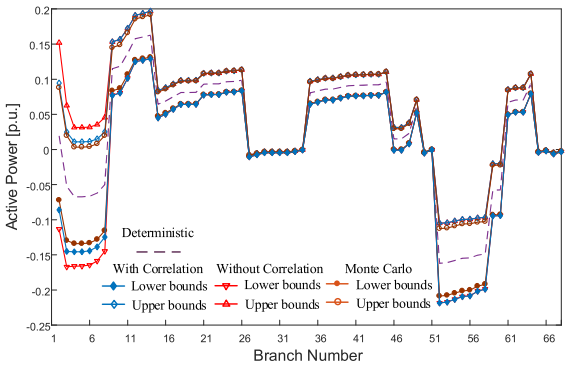

FIGURE 11. The results of active power of PG&E69-bus system.

We continue to explore the impact of uncertainty level on the bounds of the IPF solutions using the proposed method in this paper. The results are described in Fig.12. It shows

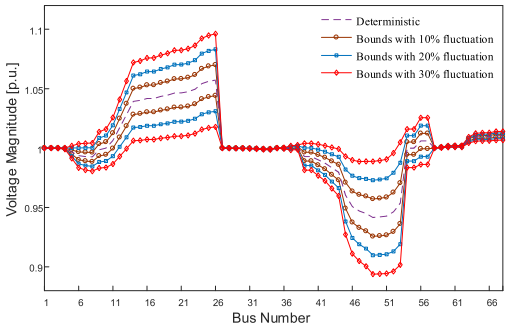

FIGURE 12. Impact of uncertainty level on voltage magnitude.

that the obtained boundaries, i.e., the bus voltage magnitude, become much tighter with decreasing of uncertainty level from 30% to 20% and 10%.

In order to indicate the optimization level of the proposed method, voltage magnitude is used as an example to define maximum, minimum and average evaluation indexes, which are shown in (32), (33) and (34).

$$A_{\max} = \max\left(\frac{v_{m,i}^{\max} - v_{m,i}^{\min}}{v_i^{\max} - v_i^{\min}}\right) \times 100\% \tag{32}$$

$$A_{\min} = \min\left(\frac{v_{m,i}^{\max} - v_{m,i}^{\min}}{v_i^{\max} - v_i^{\min}}\right) \times 100\% \tag{33}$$

$$A = \frac{\sum_{i=1}^{n} (v_{m,i}^{\max} - v_{m,i}^{\min})}{\sum_{i=1}^{n} (v_i^{\max} - v_i^{\min})} \times 100\% \tag{34}$$

where $v_{m,i}^{max}$ and $v_{m,i}^{min}$ are true upper and lower bounds of IPF, which can be represented by the MC simulation results, and v_i^{max}, v_i^{min} are estimated boundaries calculated by the AA, including the methods with correlation and without correlation. So the evaluation indexes are the ratio that the widths for interval results obtained by AA to the ones obtained by the MC method, and A is the average value, A_{max} is the maximum value and A_{min} is the minimum value. The results of IEEE118-bus distribution system is added to the simulation, because much larger grid size can be provided to validate the performance of the presented method. The injection capacity of correlated DGs and loads is 2000+j500 kVA, and the correlations of bus 85 and 88, bus 37 and 62, bus 77 and 99, bus 46 and 54, bus 113 and 118 are considered (DGs: bus 85, 88, 37, 62, 77, 99, 46, 113, Load: bus 54 and 118).

The correlated level is set as −0.15, and 10% variation of output power for generators and loads is considered. The results are shown as Table 2.

For the values of three evaluation indexes A, A_{max} and A_{min} in any one power system above. The evaluation indexes with correlations are larger than the ones of without correlation, which shows that the results obtained by the proposed method are closer to the true values according to Table 2. Moreover, the calculation time (Computer: Core(TM) i5-5200 CPU @ 2.20GHz, 8GB RAM) increases with the increasing of the scale of distribution system, and the time with correlation (3.09s, 11.66s, 32.49s for IEEE33-bus system, PG&E69-bus system, IEEE118-bus system respectively) is not much more than the time without correlation (2.09s, 10.02s, 29.27s for IEEE33-bus system, PG&E69-bus system, IEEE118-bus system respectively). These two methods are all much faster than MC (17.84s, 71.87s, and 199.55s).

For different system, we can get the same conclusion that the proposed method with correlation can narrow the IPF solutions without spending much more time.

VI. CONCLUSION

This paper proposes an improved IPF method that considers the correlations of input variables (DGs-DGs and DGs-loads) in the distribution power system based on AA, which makes the interval solutions of uncertain power flow more accurate. The distribution system that integrates DGs and loads is used as an example to validate the effectiveness of proposed method, the obtained calculation results show that the interval correlations do affect the accuracy of IPF solutions, and the bounds of interval solutions would be much tighter with correlation of input variables.

Both the correlations of DGs-DGs and DGs-loads have the effect that narrows the bounds of IPF. Furthermore, the bounds of the IPF interval results also change with different uncertainty level. Generally, much smaller the uncertainty fluctuation is, the much tighter the bounds are.

Although the method presented in this paper is proved to be practical and effective, there remains a lot of research to do, such as the nature of the interval correlation, the impact of different location and number of integrated DGs and loads, and the improvement of the correlation model.

REFERENCES

[1] A. Dimitrovski and K. Tomsovic, "Boundary load flow solutions," *IEEE Trans. Power Syst.*, vol. 19, no. 1, pp. 348–355, Feb. 2004.

[2] Z. Wang and F. L. Alvarado, "Interval arithmetic in power flow analysis," *IEEE Trans. Power Syst.*, vol. 7, no. 3, pp. 1341–1349, Aug. 1992.

[3] F. Alvarado, Y. Hu, and R. Adapa, "Uncertainty in power system modeling and computation," in *Proc. IEEE Int. Conf. Syst., Man Cybern.*, Chicago, IL, USA, Oct. 1992, pp. 754–760.

[4] R. E. Moore, "Finite representations," in *Methods and Applications of Interval Analysis*, Philadelphia, PA, USA: SIAM, 1979, pp. 9–17.

[5] R. Krawczyk, "Newton-algorithmen zur bestimmung von nullstellen mit fehlerschranken," *Computing*, vol. 4, no. 3, pp. 187–201, Sep. 1969.

[6] H. Mori and A. Yuihara, "Calculation of multiple power flow solutions with the Krawczyk method," in *Proc. IEEE Int. Symp. Circuits Syst.*, Orlando, FL, USA, Jun. 1999, pp. 94–97.

[7] A. Vaccaro and D. Villacci, "Radial power flow tolerance analysis by interval constraint propagation," *IEEE Trans. Power Syst.*, vol. 24, no. 1, pp. 28–39, Feb. 2009.

[8] L. V. Barboza, G. P. Dimuro, and R. H. S. Reiser, "Towards interval analysis of the load uncertainty in power electric systems," in *Proc. Int. Conf. Probabilistic Methods Appl. Power Syst.*, Ames, IA, USA, Sep. 2004, pp. 538–544.

[9] J. Stolfi and L. H. De Figueiredo, "Self-validated numerical methods and applications," *Amer. J. Psychiatry*, vol. 112, no. 9, pp. 673–677, Jul. 1997.

[10] L. H. de Figueiredo and J. Stolfi, "Affine arithmetic: Concepts and applications," *Numer. Algorithms*, vol. 37, nos. 1–4, pp. 147–158, Dec. 2004.

[11] A. Vaccaro, C. A. Canizares, and D. Villacci, "An affine arithmetic-based methodology for reliable power flow analysis in the presence of data uncertainty," *IEEE Trans. Power Syst.*, vol. 25, no. 2, pp. 624–632, May 2010.

[12] A. Vaccaro, C. A. Canizares, and K. Bhattacharya, "A range arithmetic-based optimization model for power flow analysis under interval uncertainty," *IEEE Trans. Power Syst.*, vol. 28, no. 2, pp. 1179–1186, May 2013.

[13] C. Zhang, H. Chen, and H. Ngan, "A Mixed interval power flow analysis under rectangular and polar coordinate system," *IEEE Trans. Power Syst*, vol. 32, no. 2, pp. 1422–1429, Jun. 2016.

[14] Y. Wang, Z. Wu, X. Dou, M. Hu, and Y. Xu, "Interval power flow analysis via multi-stage affine arithmetic for unbalanced distribution network," *Electr. Power Syst. Res.*, vol. 142, pp. 1–8, Jan. 2017.

[15] J. Luo, L. Shi, and Y. Ni, "Uncertain power flow analysis based on evidence theory and affine arithmetic," *IEEE Trans. Power Syst.*, vol. 33, no. 1, pp. 1113–1115, Jan. 2018.

[16] T. Ding, R. Bo, F. Li, Q. Guo, H. Sun, W. Gu, and G. Zhou, "Interval power flow analysis using linear relaxation and optimality-based bounds tightening (OBBT) methods," *IEEE Trans. Power Syst.*, vol. 30, no. 1, pp. 177–188, Jan. 2015.

[17] C. Duan, L. Jiang, W. Fang, and J. Liu, "Moment-SOS approach to interval power flow," *IEEE Trans. Power Syst.*, vol. 32, no. 1, pp. 522–530, Jan. 2017.

[18] X. Liao, K. Liu, and J. Le, "Review on interval power flow calculation methods in power system," *Proc. CSEE*, vol. 39, no. 2, pp. 447–458 and 642, Jan. 2019.

[19] C. Jiang, X. Han, G. Y. Lu, J. Liu, Z. Zhang, and Y. C. Bai, "Correlation analysis of non-probabilistic convex model and corresponding structural reliability technique," *Comput. Methods Appl. Mech. Eng.*, vol. 200, nos. 33–36, pp. 2528–2546, Aug. 2011.

[20] Z. Qiu, "Convex models and interval analysis method to predict the effect of uncertain-but-bounded parameters on the buckling of composite structures," *Comput. Methods Appl. Mech. Eng.*, vol. 194, nos. 18–20, pp. 2175–2189, May 2005.

[21] C. Jiang, C.-M. Fu, B.-Y. Ni, and X. Han, "Interval arithmetic operations for uncertainty analysis with correlated interval variables," *Acta Mechanica Sinica*, vol. 32, no. 4, pp. 743–752, Aug. 2016.

[22] C. Jiang, Q. F. Zhang, X. Han, and Y. H. Qian, "A non-probabilistic structural reliability analysis method based on a multidimensional parallelepiped convex model," *Acta Mechanica*, vol. 225, no. 2, pp. 383–395, Feb. 2014.

[23] H. Wang, X. Li, and B. Zou, "Probabilistic load flow calculation of distribution system based on Bayesian network to depict wind-photovoltaic-load correlation," *Proc. CSEE*, vol. 39, no. 16, pp. 4753–4763 and 4977, Aug. 2019.

[24] X. Ran and S. Miao, "Three-phase probabilistic load flow for power system with correlated wind, photovoltaic and load," *IET Gener., Transmiss. Distrib.*, vol. 10, no. 12, pp. 3093–3101, Sep. 2016.

[25] B. Venkatesh, R. Rakesh, and H. B. Gooi, "Optimal reconfiguration of radial distribution systems to maximize loadability," in *Proc. IEEE Power Eng. Soc. Gen. Meeting*, Feb. 2004, pp. 260–266.

[26] D. Zhang, T. Zhang, X. Xu, Y. Zhou, and X. Zhang, "Optimal reconfiguration of the active distribution network with distributed generation and electric vehicle," *J. Eng.*, vol. 2017, no. 13, pp. 1453–1456, Jan. 2017.

SHIPENG LENG was born in Jiangxi. He received the B.E. degree in electrical engineering from the University of Electronic Science and Technology of China, Chengdu, China, in 2017. He is currently pursuing the M.E. degree with the School of Electrical Engineering and Automation, Wuhan University, Wuhan, China. His current research interests include the interval correlation and interval power flow analysis.

KAIPEI LIU was born in Hubei. He received the Ph.D. degree in computer application technology from Wuhan University, Wuhan, China, in 2001. He is currently a Professor with the School of Electrical Engineering and Automation, Wuhan University. His current research interests include power system operation and control, smart grids, and VSC-HVDC integrated with renewable energy source.

XIAOHONG RAN (Member, IEEE) was born in Chongqing. He received the Ph.D. degree in electrical power engineering from the Huazhong University of Science and Technology, Wuhan, China, in 2015. Since 2015, he has been with the School of Electrical Engineering and Automation, Wuhan University, Hubei, China. He is currently a Visiting Researcher in the field of modeling and control for the ac/dc converters with the Georgia Institute of Technology, Atlanta, USA. His current research interests include the control of power electronics converters applied to the renewable energy technology, dc power grid/dc–dc converters, and parameter identification and interval optimization of power systems.

SHUYAO CHEN, photograph and biography not available at the time of publication.

XUNYUE ZHANG, photograph and biography not available at the time of publication.